Catalysts **2015**, *5*, 460-477; doi:10.3390/catal5010460

OPEN ACCESS

catalysts

ISSN 2073-4344

www.mdpi.com/journal/catalysts

Article

Structural Evolution under Reaction Conditions of Supported $(NH_4)_3HPMo_{11}VO_{40}$ Catalysts for the Selective Oxidation of Isobutane

Fangli Jing [1], Benjamin Katryniok [1,2], Elisabeth Bordes-Richard [1,3], Franck Dumeignil [1,4] and Sébastien Paul [1,2,*]

1 CNRS UMR 8181, Unité de Catalyse et Chimie du Solide (UCCS), Université Lille 1 Sciences et Technologies, F-59655 Villeneuve d'Ascq Cedex, France; E-Mails: fangli.jing@univ-lille1.fr (F.J.); benjamin.katryniok@ec-lille.fr (B.K.); elisabeth.bordes@univ-lille1.fr (E.B.-R.); franck.dumeignil@univ-lille1.fr (F.D.)

2 Ecole Centrale de Lille, ECLille, F-59651 Villeneuve d'Ascq, France

3 Ecole Nationale Supérieure de Chimie de Lille, ENSCL, F-59659 Villeneuve d'Ascq, France

4 Institut Universitaire de France, IUF, Maison des Universités, 103 Bd St-Michel, F-75005 Paris, France

* Author to whom correspondence should be addressed; E-Mail: sebastien.paul@ec-lille.fr; Tel.: +33-3-2033-5457; Fax: +33-3-2033-5499.

Academic Editor: Keith Hohn

Received: 24 November 2014 / Accepted: 6 March 2015 / Published: 23 March 2015

Abstract: When using heteropolycompounds in the selective oxidation of isobutane to methacrolein and methacrylic acid, both the keeping of the primary structure (Keggin units) and the presence of acidic sites are necessary to obtain the desired products. The structural evolution of supported $(NH_4)_3HPMo_{11}VO_{40}$ (APMV) catalysts under preliminary thermal oxidizing and reducing treatments was investigated. Various techniques, such as TGA/DTG (Thermo-Gravimetric Analysis/Derivative Thermo-Gravimetry), H_2-TPR (Temperature Programed Reduction), *in situ* XRD (X-Ray Diffraction) and XPS (X-ray Photoelectron Spectroscopy), were applied. It was clearly evidenced that the thermal stability and the reducibility of the Keggin units are improved by supporting 40% APMV active phase on $Cs_3PMo_{12}O_{40}$ (CPM). The partial degradation of APMV takes place depending on temperature and reaction conditions. The decomposition of ammonium cations (releasing NH_3) leads to the formation of vacancies favoring cationic exchanges between vanadium coming from the active phase and cesium coming from the support. In addition, the vanadium expelled from the

Keggin structure is further reduced to V^{4+}, species, which contributes (with Mo^{5+}) to activate isobutane. The increase in reducibility of the supported catalyst is assumed to improve the catalytic performance in comparison with those of unsupported APMV.

Keywords: isobutane; methacrylic acid; selective oxidation; characterization by *in situ* methods; heteropolymolybdates

1. Introduction

Keggin-type heteropolyacid and their salts exhibit excellent performance in several catalytic reactions like oxidation, ammoxidation [1,2], oxidative dehydrogenation [3,4] and dehydration [5,6]. More particularly, vanado-molybdo-phosphoric acid ($H_4PMo_{11}VO_{40}$) is a promising bi-functional catalyst for the direct oxidation of isobutane (IBAN) into methacrylic acid (MAA) because of its acidic and redox chemical properties [7–10]. However, the thermal stability of this catalyst, which restructures on-stream, is poor [11]. Later, it was found that the use of large cations like cesium in Keggin-type heteropolymolybdates did not only improve the microstructure of the resulting catalyst, but also enhanced its thermal stability. Among counter-cations of polymolybdates that were studied in literature, ammonium ion NH_4^+ was less often used than H^+, K^+, Cs^+ and their combinations. Paul *et al.* [12,13] were the first authors to study the ammonium salt of *11*-molybdo-*1*-vanado-phosphoric acid $(NH_4)_3HPMo_{11}VO_{40}$ (APMV) as a catalyst to synthesize methacrolein (MAC) and methacrylic acid starting from isobutane. The results showed that the catalyst was very selective to the desired products. For the same reaction, the catalytic behavior of the ammonia salt of *12*-molybdophosphoric acid, $(NH_4)_3PMo_{12}O_{40}$, was examined by Cavani's team [14,15]. They showed that the partial decomposition of ammonium was responsible for the presence of few Mo^{5+} species, the presence of which was correlated with higher selectivity. One could add that, as it is the case for V- or Mo-containing oxides used in the selective oxidation of alkanes, V^{4+} like Mo^{5+} species, could also play a role in the activation of isobutane [16]. In an attempt to increase the surface specific reaction rate, APMV was dispersed on different types of SiO_2-based supports with high surface area, and on the cesium salt of *12*-molybdophosphoric acid, $Cs_3PMo_{12}O_{40}$ (CPM). Only the latter was found to increase the catalytic performance as well as to stabilize the APMV active phase [17,18].

Indeed, from the catalytic point of view, it is mandatory to maintain the integrity of $[PMo_{11}VO_{40}]$ or $[PMo_{12}O_{40}]$ polyanions, which are known as constituting the Keggin units, also called the "primary structure". In the case of $PMo_{12}O_{40}^{3-}$, a central tetrahedral PO_4 group is spherically surrounded by twelve MoO_6 octahedra. P–O bonds are linked to four Mo_3O_{13} groups. Each Mo_3O_{13} group is formed by three edge-sharing MoO_6 and connected by corner-sharing Mo–O. One (to three) VO_6 groups may replace MoO_6 groups, as in $PMo_{11}VO_{40}^{3-}$. In the secondary structure, these Keggin units are maintained together by counter-cations including protons, and possibly water molecules at room temperature. During the catalytic reaction, water molecules may come in and out, the reason why steam is added in reactant feed to avoid the collapse of the resulting secondary structure. Owing to its thermal instability, ammonium NH_4^+ is partially eliminated as NH_3 during the pre-treatment step (calcination), as well as during the catalytic reaction. The restructuring of the solid to a stable catalyst depends on the operating conditions (temperature, atmosphere, flowrates, *etc.*). The common *ex situ* measurements, such as XRD, XPS and

other spectroscopic methods, give useful information on the catalyst before and after catalytic reaction. However, to examine how the primary and secondary structures are modified when nitrogenated species are lost during calcination and reaction, and to get information about the chemical state of surface elements under stream, *in situ* techniques were carried out. Indeed, the selective oxidation of isobutane is supposed to proceed via a Mars-Van-Krevelen mechanism [12], stating that in the first step, the catalyst is partially reduced by isobutane, whereby the latter is oxidized by the surface lattice oxygen, before being re-oxidized in the second step by co-fed molecular oxygen. The influence of oxidizing (air) and reducing (hydrogen) atmosphere on the evolution of the precursor and the calcined catalyst was studied by *in situ* XRD measurements for bulk APMV and APMV supported on CPM (40 wt.% active phase loading) (further noted APMV/CPM). Furthermore, APMV/CPM was investigated by XPS after pretreatment in isobutane atmosphere. The catalytic properties will be first recalled, as well as few results already obtained about the reactivity of samples (TGA, H_2-TPR), to allow comparison with the results of the present *in situ* study.

2. Results and Discussion

2.1. Catalytic Evaluation for Isobutane Oxidation Reaction

The catalytic results in oxidation of isobutane for the production of methacrolein and methacrylic acid are just recalled here and listed in Table 1. They were quite different when CPM, APMV and APMV/CPM catalysts were used. The CPM support was catalytically inert. Unsupported APMV exhibited a quite low activity with only 2.5% conversion and the yield in the desired products (MAC + MAA) was as low as 1.4%. By supporting 40% of APMV on CPM, the conversion of isobutane increased by more than five times, from 2.5% to 15.3%, and correspondingly, the yield to MAC + MAA also increased to 8.0%. It is well known that both acid and redox properties are indispensable to catalyze the oxidation of isobutane [19]. The important role of the acidic sites has been discussed elsewhere [17,18]. The absence of acid sites at the surface of the CPM support is responsible for its inertness. The acid and redox properties can be modified by dispersing the active phase APMV on CPM. More importantly, a dynamical surface restructuration, which will be discussed in the present paper, may exist under reaction conditions for the supported sample. Furthermore, the supported catalyst APMV/CPM has proved an excellent stability under stream during 132 h [18].

Table 1. Catalytic performances for selective oxidation of isobutane over the different samples.

Catalyst	Conversion, % [a]		Selectivity, %				$Y_{(MAC+MAA)}$, %	Carbon balance, %
	O_2	IBAN	MAC	MAA	CO_x	Others		
CPM	-	-	-	-	-	-	-	100.0
APMV	10.7	2.5	20.4	34.3	35.8	9.5	1.4	99.7
APMV/CPM	61.6	15.3	10.0	42.0	30.7	17.3	8.0	99.3

[a] Reaction conditions: Temperature = 340 °C, atmospheric pressure, contact time = 4.8 s, IBAN/O_2/H_2O/inert = 27/13.5/10/49.5 (molar ratios). IBAN = isobutane, MAC = methacrolein, MAA = methacrylic acid; others products include acetic acid and acrylic acid.

2.2. Reactivity of the Precursors of APMV and APMV/CPM in Air

2.2.1. Thermal Decomposition

The main results of the TGA-DTG study [18] will just be recalled here, to be further correlated with new TP-XRD experiments. The physisorbed and crystal water were lost up to T_{pret} = 160 °C for unsupported APMV precursor, and up to 200 °C when APMV precursor was supported on CPM (Figure 1). This is a first demonstration of the stabilizing effect of CPM support. Upon increasing temperature, the decomposition of ammonium cations to ammonia (and water) and loss of proton (with formation of water) happened in the 250–424 °C range for APMV and 245–402 °C for APMV/CPM. These signals were immediately followed by a slight gain of weight (but strong DTG signal), which was assigned to the reoxidation of V^{4+} (generated by the decomposition of ammonium to NH_3) to V^{5+} species at 424 °C (APMV), and at 402 °C for APMV/CPM. Thus, all temperatures, except those for H^+ loss and V^{4+} reoxidation, were the lowest for supported APMV. Between 450 °C and 640 °C the weight remained constant and it corresponded to the formation of Keggin-type compound with oxygen vacancy, called $PMoV_{11}O_{38}$ [20]. Indeed in the 250–500 °C range, the weight loss during the transformation of anhydrous APMV to $PMo_{11}VO_{38}$ was 5.0% (theoretical value 4.8%). In the case of 40% APMV supported on CPM the observed weight loss was only 0.9%, instead of the theoretical 1.92% value. These experiments suggest that the thermal stability of APMV was globally improved when supported on CPM. At higher temperatures, the decomposition led to P, V, Mo oxides, followed by the beginning of sublimation of phosphorus oxide and MoO_3.

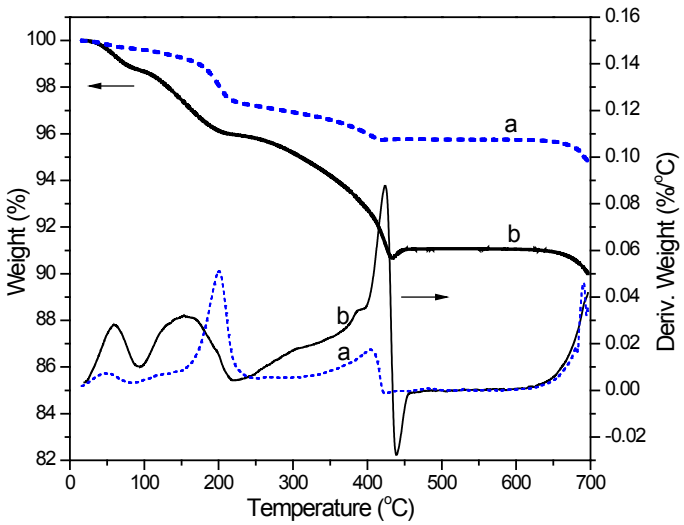

Figure 1. TGA (Thermo-Gravimetric Analysis) and DTG (Derivative Thermo-Gravimetry) curves of the fresh samples (precursors) heated in air (a: APMV/CPM and b: bulk APMV).

Therefore, at the temperature of 350 °C chosen for calcination of the precursor, it is expected that some ammonium ions remain in the secondary structure, and that most vanadium species are V^{5+}-type. Both $(NH_4)_3HPMo_{11}VO_{40}$ and $H_3PMo_{11}VO_{40}$ particles may coexist, and/or solid solutions of $(NH_4)_{3-x}H_xPMo_{11}VO_{40}$ type may be present in APMV, while things are more complicated for APMV/CPM, as shown further.

2.2.2. Temperature-Programmed XRD in Air

TP-XRD experiment was carried out up to 400 °C on APMV precursor (Figure 2). At room temperature (R.T.), the diffraction lines of the cubic structure typical of Keggin-type heteromolybdates were found at 2θ = 10.8°, 18.8°, 24.3°, 26.6°, 30.9°, 36.3° and 39.6° [21,22]. The presence of $(NH_4)_3HPMo_{11}VO_{40}$ was demonstrated by the two characteristic lines, which clearly appeared at 2θ = 15.3° and 21.7° (triangle down in Figure 2). Some changes were detected upon heating, which consisted of shifting of diffraction lines to lower angles. An example is given for the strongest (222) diffraction line (Figure 2, right). As long as ammonium decomposed, it shifted quite regularly up to 300 °C (from 2θ = 26.7° at R.T. to 26.45° at 300 °C). Then it decreased up to 26.1° at 400 °C (Figure 3), a value characteristic of the (222) line of anhydrous $H_3PMo_{12}O_{40}$. The shift to lower diffraction angles is accounted for the fact that during the transformation of $(PMo_{11}VO_{40})^{4-}$ to $[(PMo_{12}O_{40})^{3-} + V]$, the *d*-spacing increases (θ decreases) because the cationic radius of Mo^{6+} is bigger (0.59 Å) than that of V^{5+} (0.54 Å). Initiated by the loss of ammonium cations as ammonia, which is accompanied by the expulsion of vanadium from the primary structure, this transformation requires the reorganization of Mo atoms between Keggin units in order for the expelled V to be compensated.

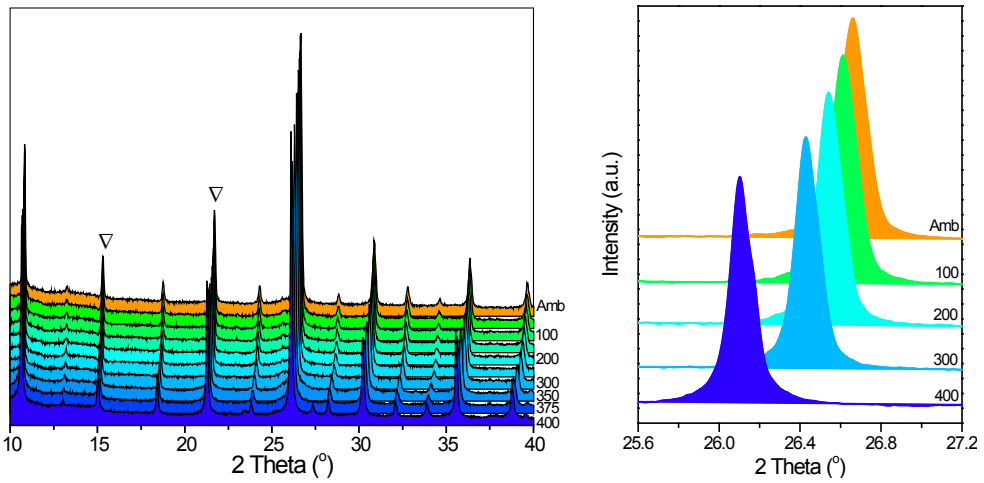

Figure 2. *In situ* XRD (X-Ray Diffraction) in air from ambient to 400 °C for the fresh APMV sample, (**left**) full range; (**right**) (222) line of APMV.

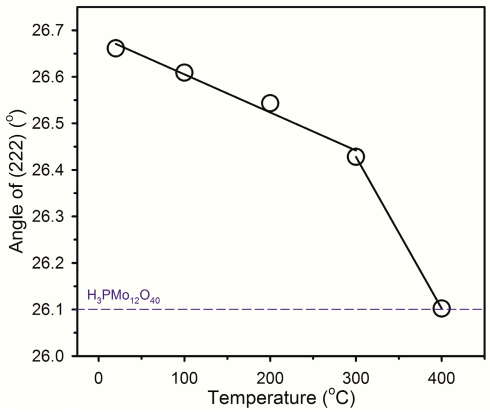

Figure 3. Variation of diffraction (222) line with an increasing temperature from ambient to 400 °C.

When the temperature increased further to 425 °C, significant changes in the crystalline phases took place (Figure 4). The characteristic lines originating from the primary structure disappeared at the expense of new diffraction lines assigned to the metal oxides or mixed-metal oxides. As an example, the pattern obtained at 425 °C exhibited diffraction peaks at 2θ = 12.4°, 23.4°, 27.3°, 33.0° and 33.9°, which were attributed to MoO_3 (diamonds in Figure 4). The lines of Mo_4O_{11} suboxide, written $(Mo_3^{6+}Mo^{4+})O_{11}$ (asterisks in Figure 4), were also found at 22.9° and 24.9°, but they disappeared when the temperature reached 500 °C. The formation of this mixed valence oxide is the result of the effect of ammonia release, which, here, reduces Mo^{6+} partly to Mo^{4+}. On the contrary, the shoulder at 25.1°, which is really ill defined (arrows in Figure 4), evolved to a distinguishable diffraction peak. Therefore, Mo_4O_{11} can be considered as an intermediate during the structural evolution. The lines of V_2O_5 (or V_2O_4) were not observed but there are several reasons for that, beginning by the relatively small amount of V in the sample.

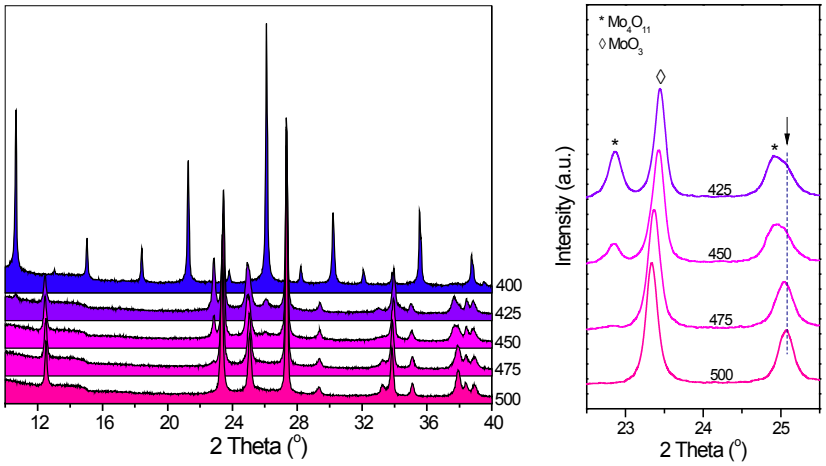

Figure 4. *In situ* XRD from 400 °C to 500 °C for fresh APMV (precursor), (**left**) full range; (**right**) diffractions from molybdenum oxides (*: Mo_4O_{11}, ◊: MoO_3).

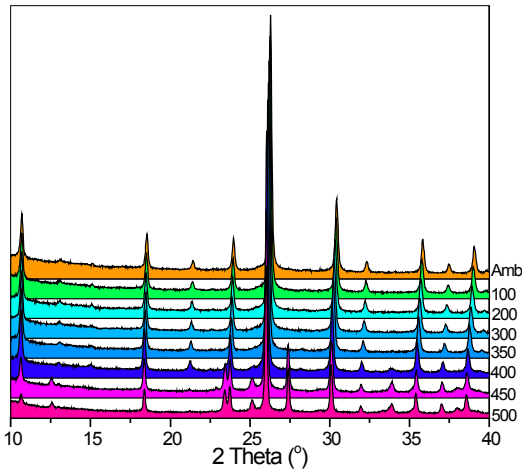

Figure 5. *In situ* XRD in air for the supported sample APMV/CPM.

In the case of CPM-supported APMV, its structural evolution followed by TP-XRD in air illustrated again the greater stability of supported APMV. At R.T. the diffraction lines were characteristic of the cubic structures of both CPM and APMV. The two characteristic lines of APMV (2θ = 15.3° and 21.7°) were more difficult to see due to 40% APMV/CPM. As temperature increased, lines shifted to low angles

and accounted for the presence of $H_3PMo_{12}O_{40}$/CPM. The lines were present up to 500 °C instead of 375 °C for AMPV (Figure 5). From 400 to 500 °C, the weak diffraction peaks from MoO_3 at 27.3° and from Mo_4O_{11} at 22.9° and 24.9° were superimposed to those of the cubic structure.

2.3. Reducibility of Calcined Catalysts in Hydrogen Atmosphere

2.3.1. Temperature Programmed Reduction H_2-TPR

H_2-TPR measurements on CPM, APMV and APMV/CPM catalysts were performed to investigate the influence of the support on the reducibility of the catalytically active APMV phase (Figure 6). Almost no hydrogen consumption peak could be found for the bare CPM support but some Mo^{5+} species probably began appearing above 620 °C. Four main steps were distinguished in the reduction profile after deconvolution treatment, which were tentatively assigned in Table 2 to the successive reductions of V and Mo. Obviously the reduction of species, e.g. Mo^{6+} to Mo^{5+}, may begin before completion of the V^{4+} to V^{3+} step. Indeed it is well-known that vanadium is reduced before molybdenum when these species are present in the same oxidic compound [23]. Thus, the slight but long reduction at *ca.* 500–600 °C would be attributed to the reduction of vanadium species. The decomposition of ammonium ions, which initiated the expulsion of vanadium from Keggin units, was probably delayed in hydrogen atmosphere as compared to air, but above 550 °C it could be expected that most V species have moved in between $PMo_{12}O_{40}$ units. The reduction of Mo^{4+} to lower oxidation states might proceed above 650 and 690 °C for APMV/CPM and APMV, respectively.

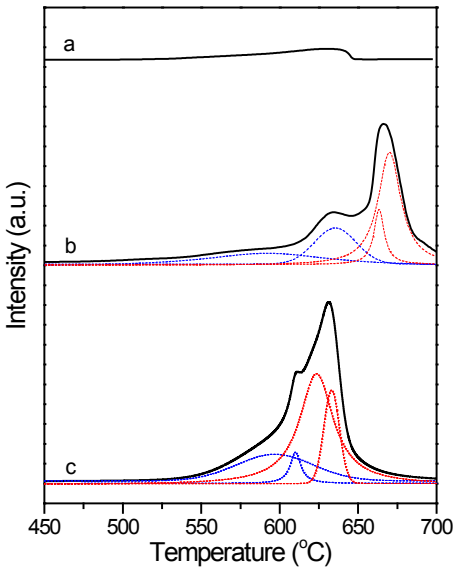

Figure 6. TPR (Temperature Programed Reduction) profiles of: (**a**) CPM; (**b**) APMV; and (**c**) APMV/CPM catalyst (Blue lines: reduction of V species, red lines: reduction of Mo species).

The main hydrogen consumption at 640–690 °C for APMV catalyst was ascribed to the reduction of Mo^{6+} to Mo^{4+} [9]. Furthermore, according to the quantitative calculation of consumed hydrogen in Table 2, the supported sample APMV/CPM consumed 1.2 times more hydrogen than APMV alone, and the reduction of Mo^{6+} to Mo^{4+} exhibited higher hydrogen consumption than reduction of V^{4+} to V^{3+} for both samples.

When compared to APMV, it was observed that the reduction steps occurred at higher temperature than for that CPM-supported APMV. In other words, the reducibility of the supported catalyst was improved. On the other hand, not only the temperature of reduction was lowered, but also more metallic ions were reduced by supporting APMV.

Table 2. Tentative attribution of H_2-TPR signals for APMV and APMV/CPM.

Temperature range, °C		H_2 Consumption, mmol/g		Attribution
APMV	APMV/CPM	APMV	APMV/CPM	
500–650 (587) [a]	575–650 (595)	1.09	1.14	Reduction of V^{5+} to V^{4+}
580–670 (635)	590–625 (610)	0.84	0.27	Reduction of V^{4+} to V^{3+}
640–690 (663)	580–700 (623)	0.46	2.95	Reduction of Mo^{6+} to Mo^{5+}
600–700 (670)	610–650 (632)	1.96	0.81	Reduction of Mo^{5+} to Mo^{4+}

[a] peak maximum in parentheses.

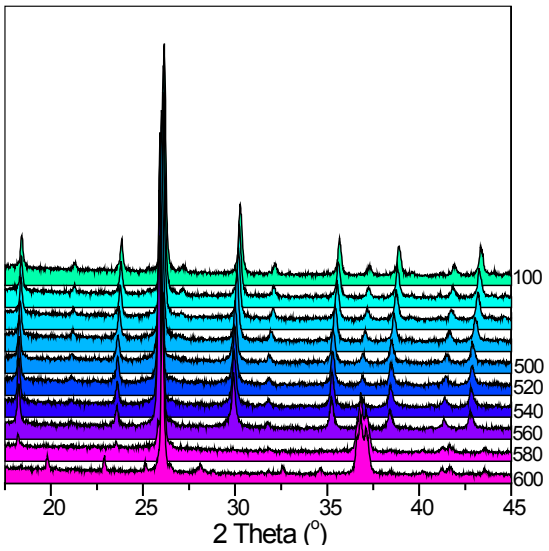

Figure 7. *In situ* XRD under hydrogen for the supported APMV/CPM catalyst.

2.3.2. TP-XRD of APMV/CPM under Hydrogen Atmosphere

To be correlated with the H_2-TPR results, the structural evolution of APMV/CPM under reductive atmosphere was studied by *in situ* H_2-TP-XRD (Figure 7). The diffraction lines assigned to the cubic structures of APMV and/or CPM phases observed at R.T. were maintained up to 560 °C. The intensity of the weak line at 2θ = 21.4°, which is characteristic of APMV, decreased upon increasing temperature, but it was still visible. Though it suggests a gradual decomposition of APMV, it is worth noting that in air (TP-XRD) (Figure 5) this line became weak above 400 °C and disappeared totally at 500 °C. Therefore, when supported, the Keggin structure (whatever its composition) is significantly stabilized under a reductive atmosphere, compared to an oxidative environment. Upon increasing temperature to 580 °C, the Keggin structure collapsed, as shown by the very different and new diffractograms. No formation of $PMo_{11}VO_{38}$ could be demonstrated. The formation of metal oxides and suboxides formed by reduction was directly put in evidence. The strong diffraction line at 2θ = 26.0° and the lines at 2θ = 36.8° and 53.5° were assigned to MoO_3 and MoO_2, respectively. This finding is in good agreement with H_2-TPR results showing an overlapped reduction peak from 550 °C to 650 °C. Lines at 2θ = 37.1° and 52.6° were assigned to V_2O_4

generated by V_2O_5 reduction. When the temperature reached 600 °C, several new diffraction peaks at low angles (16.1°, 19.8°, 23.0°, 28.1° and 28.8°) became visible, but they could not be attributed without ambiguity. They could originate from one or more mixed oxides, such as MoP_xO_y and VP_xO_y. Except the reduction of vanadium, the decomposition process was in good agreement with that suggested by TGA/DTG in air (Figure 1).

As a partial conclusion, the main findings about the reduction behavior of APMV and APMV/CPM studied by H_2-TPR and H_2-TP-XRD are: (i) the Keggin structure (in the form of APMV, $H_4PMo_{11}VO_{40}$ and/or $H_3PMo_{12}O_{40}$ + V) was stable up to *ca.* 560 °C against a deep reduction (leading to the transformation to oxides); (ii) the decomposition of the Keggin units was delayed as compared to the case of oxidative conditions where it began at *ca.* 400 °C; and (iii) the CPM support promoted the reduction of APMV.

2.4. XPS after Pretreatment under Isobutane

The composition and chemical state of the species in the first layers have already been studied for catalysts before (calcined catalysts) and after (used catalysts) the catalytic experiments by "*ex situ*" XPS technique [18]. It felt necessary to perform XPS experiments on calcined 40%APMV/CPM after pretreatement under isobutane atmosphere, to gain more information on the effects of one of the reactants on the catalyst surface (Tables 3 and 4). Values obtained in a former study by *ex situ* XPS for the same catalyst but after catalytic reaction were added for further comparison [18].

Table 3. Binding energy and surface atomic composition of 40 APMV/CPM pretreated under isobutane at various temperatures.

Temperature, T_{pret} °C	Binding energy, BE, eV			Atomic ratio [a]	Surface atomic composition
	Cs3d$_{5/2}$	P2p	O1s	O1s(1)/O1s(2)	Cs/O/P/Mo/V/N
R.T. [b]	724.0	133.9	530.7/531.9	76/24	1.9/36.6/1.1/11.0/0.8/3.4
340	723.8	133.3	530.7/531.9	84/16	1.5/37.0/1.2/11.0/0.7/1.6
540	725.2	133.8	530.7/532.1	71/29	7.4/32.8/2.2/11.0/0.1/0
560	725.2	133.7	530.7/532.1	73/27	5.4/30.5/1.9/11.0/0.1/0
580	725.2	133.7	530.7/532.1	70/30	5.9/29.1/2.1/11.0/0.1/0
R.T., post-reaction [c]	724.3	133.6	-	-	2.0/–/1.0/11/0.8/1.0

[a] Ratio of photopeak area; [b] R.T. = room temperature; [c] from [18].

Table 4. Surface analysis results for V and Mo.

Temperature, T_{pret}, °C	Binding energy, eV				Molar ratio
	V2p$_{3/2}$	Mo3d$_{3/2}$/Mo3d$_{5/2}$			
	V^{5+}/V^{4+}	Mo^{6+}	Mo^{5+}	Mo^{4+}	V^{5+}/V^{4+}
R.T. [a]	517.8/516.0	236.2/233.1	-	-	88/12
340	516.9/515.9	236.3/233.0	234.9/231.8	-	46/54
540	~516.3	236.1/232.9	234.9/231.4	233.3/229.9	0
560	~516.0	235.7/231.6	234.2/230.4	233.1/229.8	0
580	~515.8	236.2/232.9	234.5/231.3	233.2/229.8	0
R.T., post-reaction [b]	518.1/517.0	–/233.2	-	-	29/71

[a] R.T. = room temperature; [b] from [17].

The binding energies (BE) of N1s, $Cs3d_{5/2}$, P2p and O1s photopeaks and the surface composition expressed as atomic ratios are gathered in Table 3. $Cs3d_{5/2}$ and P2p photopeaks at 724 eV and 133.7 eV were assigned to Cs^+ and P^{5+} ions, respectively. The BE of P^{5+} did not change much upon temperature increase between R.T. and 560 °C, whereas *ca.* 1 eV of deviation was observed for Cs^+ photopeak. Typically, 724 eV stands for CsOH, meaning that the surface would be hydroxylated. The nitrogen N1s photopeak was found at *ca.* 402 eV (NH_4^+ ion) as a shoulder in the $Mo3p_{3/2}$ peak located itself at *ca.* 398 eV. After decomposition of the spectrum collected at room temperature, the BE of N1s could be found at 402.5 eV (Figure 8). The N1s peak became much broader at 340 °C and the surface content of N decreased by more than 50% (Table 3). At 540 °C, it disappeared while a new nitrogen species appeared at *ca.* 396.1 eV. The latter was assigned to oxynitride species [24,25]. In the case of Mo and V, the $Mo3d_{3/2}$, $Mo3d_{5/2}$ and $V2p_{3/2}$ photopeaks were decomposed to put in evidence the reduction states after pretreatment (*vide infra*) (Table 4). At room temperature, the two well-separated peaks at 236.2 eV ($Mo3d_{3/2}$) and 233.1 eV ($Mo3d_{5/2}$) were assigned to Mo^{6+} species linked to P^{5+} [26]. The wide peak at *ca.* 518 eV ($V2p_{3/2}$) was assigned to V^{5+}. This value was too high as compared to that of V_2O_5 (BE *ca.* 516.5–516.9 eV) but it was closer to those of vanadium phosphates [27,28]. In a way, the BEs for Mo and V confirmed that the Keggin structure [$PMo_{11}VO_{40}$] or [$PMo_{12}O_{40}$] was present at R.T. and at 340 °C. The O1s peak was asymmetric at any temperature. After decomposition, two species O1s(1) and O1s(2) appeared at 530.7 eV and 531.9–532.1 eV, respectively, which could be attributed to oxygen bonded to Mo and P when both are present in the same compound [26].

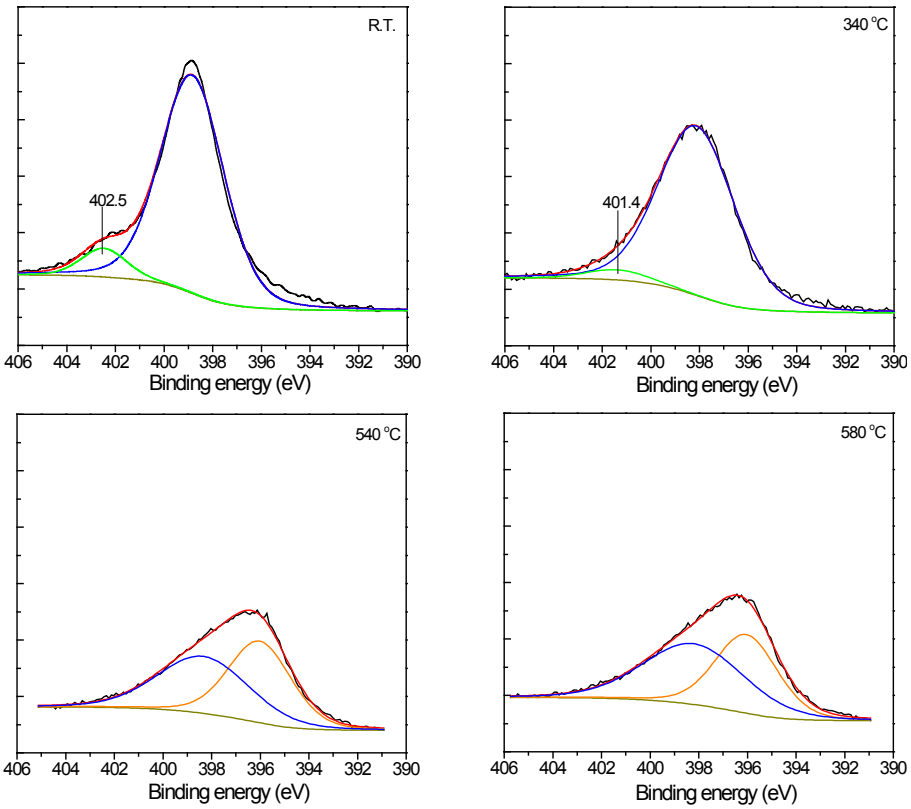

Figure 8. *In situ* XPS N1s for the APMV/CPM sample treated under isobutane.

Before examining the oxidation states of Mo and V, let us focus on the relative atomic ratios (Table 3) of N, Cs, P and their variation with T_{pret}. Significant changes could be observed upon increasing T_{pret} and

particularly when it exceeded 340 °C. The surface proportions of Cs and P significantly increased, at variance of O and V proportions. The total oxygen content decreased more and more, as expected in a reduction process, while the surface P^{5+} species increased, particularly at $T_{pret} \geq 540$ °C. This is often observed for these labile species in mixed P, V oxides [27,29]. Together with the formation of oxynitrides, the results indicated that a complex change took place at the surface at these temperatures. In the case of the used catalyst (post-reaction) examined at R.T. [18], there was no more nitrogen, but the other values were similar to those found at R.T. in the presence of IBAN.

At 340 °C which is in the temperature range of the catalytic reaction, the surface nitrogen (as NH_4^+) decreased from 3.4 at R.T. (theoretical N/Mo = 3/11) to 1.6. This decrease confirms the partial decomposition of the ammonium cations followed by ammonia release. At $T_{pret} \geq 540$ °C, all NH_4^+ disappeared, in line with TP-XRD in H_2. At variance, Cs amounts first decreased from 1.9 to 1.5 at 340 °C (theoretical value Cs/Mo = 0/11), and increased up to 5.9 above 540 °C. Vanadium also underwent a change, decreasing strongly by a tenth of its value (initially V/Mo = 1/11) at $T_{pret} \geq 540$ °C, but below 540 °C it was approximately constant. These experiments show that the expulsion of V from the primary Keggin structure [30] may happen above 340 °C, followed by the diffusion of V from the surface to the bulk.

According to the preparation procedure for 40 wt. % APMV, the support CPM ($Cs_3PMo_{12}O_{40}$) should be covered by the active phase. Actually, the opposite trend of Cs and N when the temperature increased (up to 340 °C) was in favor of the formation of the solid solution $Cs_x(NH_4)_{3-x}HPMo_{11}VO_{40}$, which was studied in a former paper [18]. The redistribution of the surface elements especially for Cs and V with temperature suggested a cationic exchange between the CPM support and the APMV active phase. The release of ammonia resulted in a protonated intermediate, which was unstable. In air, it evolved towards a lacunary Keggin-type compound by losing constitutional water (protons plus oxygen). Hence, the cesium cations compensated the loss in ammonia (or, more precisely, the loss of protons from the resulting intermediate). Above 340 °C, when there was no more ammonium, the increase of Cs/Mo from 1.5 to 7.4/11, resulting in a Cs-enriched surface as if the CPM support—*i.e.*, the bulk of the catalyst—was alone. However it was more probable that the solid was made of a mixture of oxides and suboxides. Therefore *in situ* XPS experiments confirmed that, though isobutane was a milder reducing agent than hydrogen, the Keggin structure was quite maintained in APMV/CPM up to 340 °C but that it disintegrated above 500 °C.

It is known that the redox properties of *12*-phosphomolybdic acid significantly change upon replacing one Mo by V atom in the Keggin unit [31]. Hence, the oxidation state of V is of high interest. The evolution of $V2p_{3/2}$ photopeaks is shown in Figure 9 and the quantification results are reported in Table 4. The wide peak at *ca.* 518 eV recorded at room temperature accounted for two different oxidation states of vanadium. The decomposition of the signal was done by assigning BEs at 517.8 eV and at 516.0 eV to V^{5+} and V^{4+}, respectively. The V^{5+}/V^{4+} ratio increased with T_{pret}. Thus not only vanadium was eliminated from the primary structure, but it was also reduced at the same time. In the case of $Cs_xH_{4-x}PVMo_{11}O_{40}$, the reduction was explained by an auto-reduction process within the catalyst, the O^{2-} lattice oxygen being simultaneously oxidized to O_2 [32]. However, in our case, the explanation lies in the elimination of ammonium, which is oxidized to ammonia by means of lattice oxygen, with concomitant reduction of V and/or Mo. When the temperature was increased to 340 °C, a clear shift of the main peak (pink curves in Figure 9) was observed. At the same time, the $V_{2p3/2}$ peak became less intense and much

broader compared with that observed at room temperature, indicating that the V^{5+} species were reduced to V^{4+} by isobutane (Figure 9). The calculation of V^{5+}/V^{4+} showed that the amount of V^{4+} species increased significantly from 11.9% to 53.6%. On the other hand, the decrease in the peak area suggested that the amount of the V surface species decreased. At 540 °C, the very small $V2p_{3/2}$ peak was detected at around 516 eV, which was assigned to V^{4+} species. The comparison with the same catalyst, but after reaction [17], shows that the proportion of V^{4+} was greater.

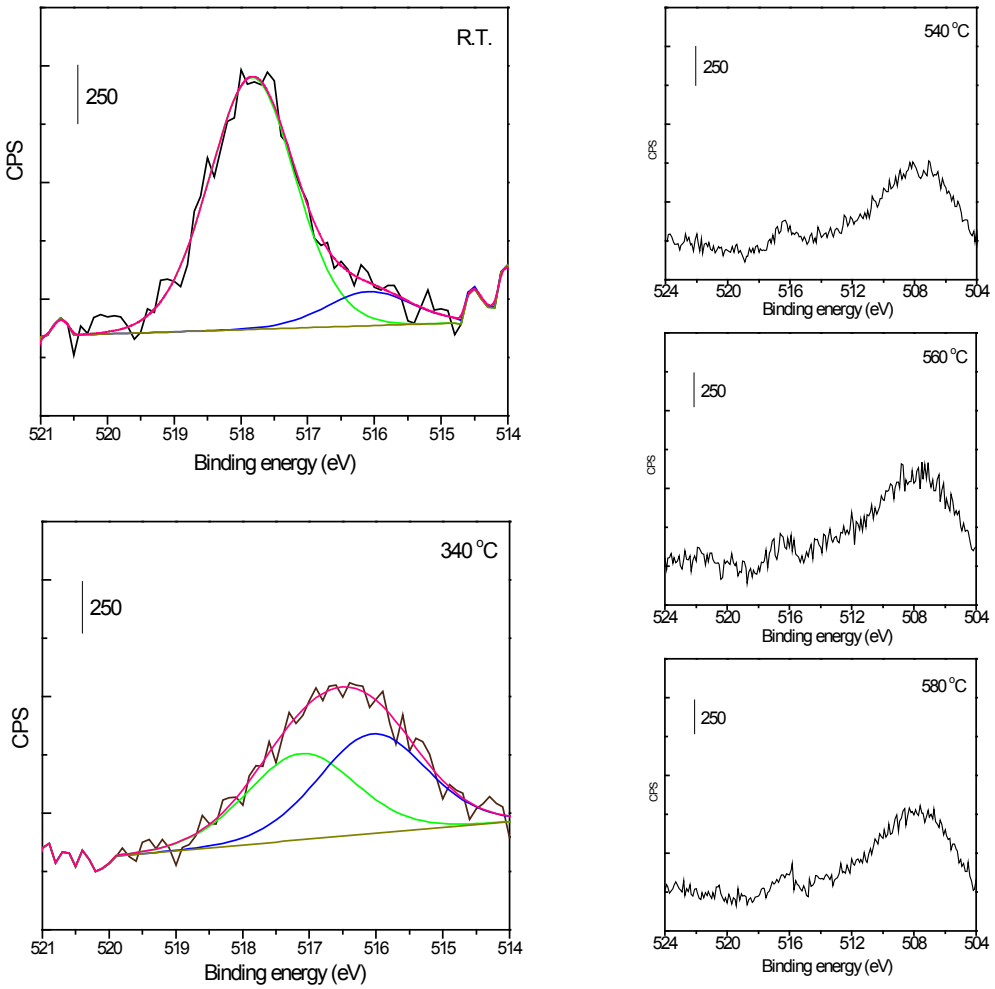

Figure 9. $V2p_{3/2}$ peaks obtained in isobutane atmosphere for the APMV/CPM sample (black: original spectrum, pink: accumulative curve, green: V^{5+} and blue: V^{4+}).

The Mo species were also reduced, as shown by the decomposition of $Mo3d_{3/2}$ and $Mo3d_{5/2}$ photopeaks at $T_{pret} \geq 340$ °C (Figure 10). The two well-separated peaks, observed at R.T. at 236.2 and 233.1 eV, respectively, tended to overlap and to shift to lower BEs when T_{pret} increased. Two new peaks appeared at 234.9 eV and 231.8 eV, which were attributed to Mo^{5+} species (green curves). Mo^{5+} was reduced to Mo^{4+} (orange curves) at 540 °C, so that the three oxidation states of molybdenum coexisted at the surface. A further increase in temperature did not affect the Mo signal, suggesting thereby that a "steady state" was obtained. BEs of Mo are close to those of MoO_3, like in MoO_3-P_2O_5 glasses containing high amounts of Mo [23].

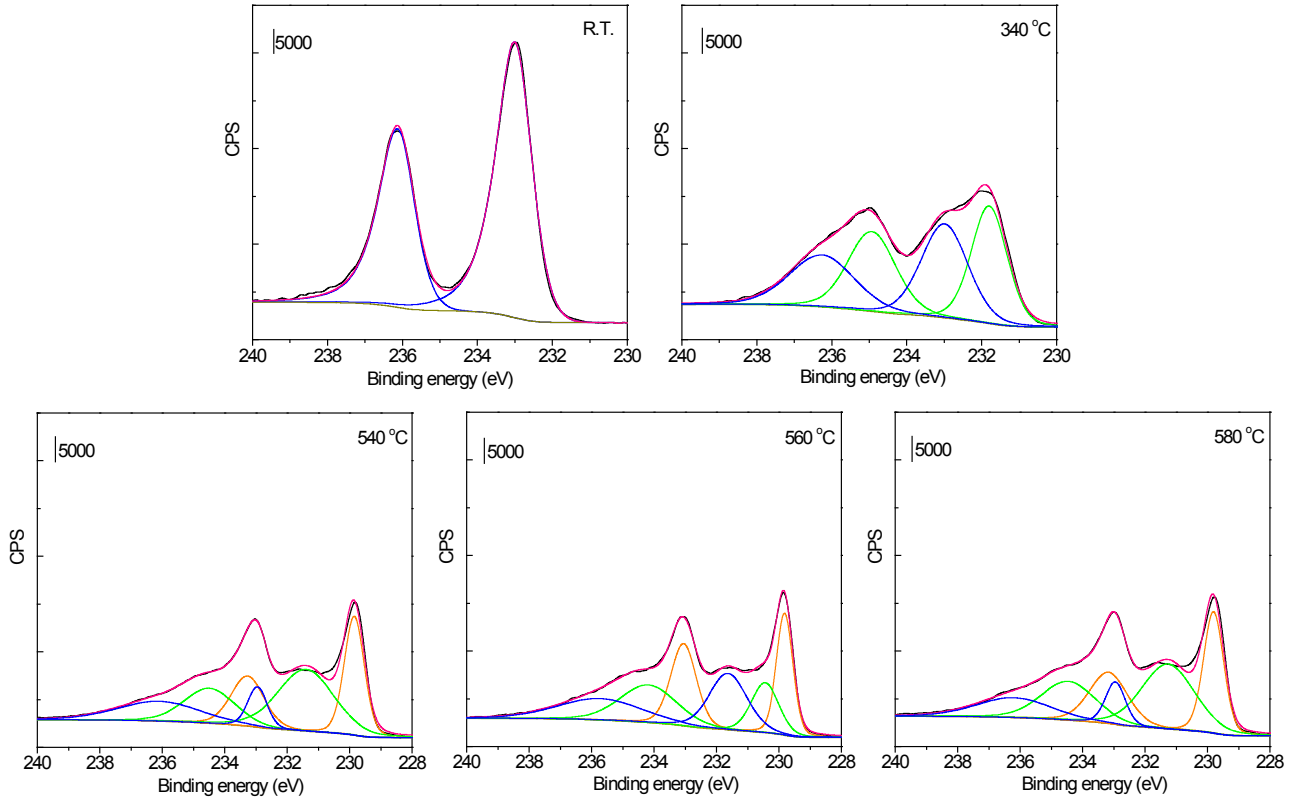

Figure 10. Reduction process of Mo species under isobutane observed by *in situ* XPS (black: original curve, pink: accumulative curve, blue: Mo^{6+}, green: Mo^{5+} and orange: Mo^{4+}).

As a conclusion, these XPS experiments after pretreatment in isobutane confirmed that not only V but also Mo species can undergo reduction and thus participate in the redox mechanism at 340 °C. They also put forth evidence of the complex restructuration of the surface. The APMV phase evolved by releasing NH_3 issued from the decomposition of ammonium cations. The resulting acidic intermediate (that could not be isolated during the experiments) rapidly loses the remaining protons, whereby the charge disequilibrium is compensated by cesium migration from the CPM support. The vanadium is expelled from the Keggin unit and then reduced by isobutane, leading to mixed-valence V species. Besides these observations, it was remarkable to find that Mo^{6+} can also be reduced to Mo^{5+} even at temperatures as low as 340 °C. Nevertheless, the consecutive reduction to Mo^{4+}—corresponding to the decomposition of the primary structure—was not observed at 340 °C but only above 540 °C. It is noteworthy that the reduction of Mo species was not observed in our "*ex situ*" XPS experiments [18]. In the spectra of calcined and used APMV/CPM samples, the BE of Mo photopeak was constant at 233.3–233.4 eV. The proportions of Cs, N and V had more or less decreased after reaction while P was quite constant (P/Mo = 1.0–1.1/11). For 11 Mo, the relative ratios were Cs/V/N = 2.0/0.8/1.0 before and 1.5/0.7/0.7 after reaction. With *in situ* XPS, Cs/V/N = 1.9/0.8/3.4 at R.T. and 1.5/0.7/1.6 at T_{pret} = 340 °C, with similar values for P. Thus the main difference lies in the proportion of nitrogen, which is higher in reducing conditions than after reaction. As stated above after H_2-TPXRD, the stability of the Keggin structure is increased in reducing conditions. The absence of Mo^{5+} in samples after reaction may be caused by (I) the reoxidation of the surface as the used catalyst was exposed to air, and/or (II) the rapid reoxidation of Mo in the operating conditions of IBAN selective oxidation.

3. Experimental Section

3.1. Material Syntheses

The hydrated *11*-molybdo-*1*-vanadophosphoric heteropolyacid ($H_4PMo_{11}VO_{40}\cdot xH_2O$) was synthesized according to a method described previously in the literature [2]. The number of crystal water molecules was calculated from TGA results (*vide infra*), which suggested that eight molecules of water were incorporated in the secondary structure ($H_4PMo_{11}VO_{40}\cdot 8H_2O$). The anhydrous acid will further be noted HPMV.

$(NH_4)_3HPMo_{11}VO_{40}$ (APMV) was prepared by co-precipitation at 45 °C, using stoichiometric amounts of NH_4NO_3 (Sigma-Aldrich, Lyon, France) and $H_4PMo_{11}VO_{40}\cdot 8H_2O$ as precursors [17]. The resulting precipitate was dried at 70 °C to obtain the APMV precursor. The APMV catalyst was obtained by calcination in static air at 350 °C (heating rate 2 °C/min) for 3 h.

The cesium salt of *12*-molybdophosphoric acid, employed as a support in the following, was prepared by controlled precipitation method [17]. An appropriate amount of Cs_2CO_3 (Sigma-Aldrich) was dissolved in water (0.1 M) and pumped into a 0.1 M aqueous solution of $H_3PMo_{12}O_{40}$ (Sigma-Aldrich) under vigorous stirring at 45 °C, generating a yellow suspension. After 2 h, the solid was recovered by removing the water under reduced pressure at 70 °C, and then dried at the same temperature for 24 h. It was finally calcined in static air at 350 °C (2 °C/min) for 3 h to obtain the solid $Cs_3PMo_{12}O_{40}$, further used as the support of APMV.

The as-prepared support was then impregnated by APMV using a deposition-precipitation method [18] as follows: CPM particles were suspended in 35 mL deionized water at 45 °C under vigorous stirring for 1 h. Then, aqueous solutions containing stoichiometric amounts of NH_4NO_3 (Sigma-Aldrich) and $H_4PMo_{11}VO_{40}$ (*i.e.*, (NH_4NO_3):$(H_4PMo_{11}VO_{40})$ = 3:1 (molar ratio)) were simultaneously pumped into the suspension to provoke APM precipitation so as to get 40 wt.% of loaded APMV. The solid noted APMV/CPM was recovered by filtration and dryness after reacting for 2 h. The conditions of calcination remained the same as for the CPM preparation.

3.2. Characterization Methods

Thermogravimetric analysis (TGA/DTG) was performed using a TA instruments (New Castle, PA, USA) 2960 SDT to study the thermal decomposition of the fresh catalyst. The samples were heated in an air flow from room temperature to 700 °C with a ramp of 3 °C/min [18].

The crystalline phases were detected by X-ray diffraction (XRD) technique on Bruker D8 Advance diffractometer (Bruker AXS, Billerica, MA, USA), using Cu Kα radiation (λ = 1.5418 Å) as an X-ray source. The reactivity of samples was studied by temperature-programmed XRD (TP-XRD) in air or hydrogen. The patterns were collected from 2θ = 10° to 60° with steps of 0.02° and an acquisition time of 0.5 s. When the measurements were carried out in air, the samples were heated in an airflow from room temperature (R.T.) to 500 °C at 1.5 °C/min heating rate, or in a reductive atmosphere (3 mol% H_2 in N_2) from R.T. to 600 °C at 10 °C/min heating rate.

The "*in situ"* surface analysis by X-ray photoelectron spectroscopy (XPS) was performed on a Kratos Axis Ultra DLD (Manchester, UK) apparatus equipped with a hemispherical analyzer and a delay-line detector. The experiments were carried out using an Al mono-chromated X-ray source (10 kV, 15 mV)

with a pass energy of 40 eV (0.1 eV/step) for high-resolution spectra and a pass energy of 160 eV (1 eV/step) for the survey spectrum in the hybrid mode and slot lens mode, respectively. The measurements were performed as follows: the sample was first heated up to the required temperature of pretreatment (T_{pret} = 340, 540, 560 and 580 °C) in diluted isobutane (5 mol% isobutane in He) at 5 °C/min heating rate, then it was transferred into the analytic chamber by an interior mechanical arm to avoid any contact with ambient air. The spectra were collected after pretreatments. A blank experiment consisted of analysis of the calcined sample (without pretreatment).

The reducibility of the catalysts was evaluated by temperature-programmed reduction under hydrogen (H_2-TPR) at atmospheric pressure. One hundred milligrams of sample were loaded in a quartz reactor and pre-treated in He flow (30 mL/min) at 100 °C for 2 h. Then, helium was replaced by the reducing gas (5 mol% H_2 in He) at the same flowrate. The temperature of the reactor was increased linearly from 100 to 800 °C at a rate of 5 °C/min. The effluent gas was analyzed by a thermal conductivity detector (TCD).

3.3. Catalytic Oxidation of Isobutane

The catalytic selective oxidation of isobutane to methacrolein and methacrylic acid was performed in a fixed-bed reactor at atmospheric pressure [21]. The catalyst (0.8 g), diluted with an equal volume of SiC (0.21 mm particle size), was loaded in a stainless-steel reactor, which was then heated up to the reaction temperature (340 °C) with a ramp of 5 °C /min under airflow (10 mL/min). Then, the airflow was replaced by the reactants (IBAN/O_2/H_2O/He = 27/13.5/10/49.5 molar ratio) fed at a total flowrate of 10 mL/min. The light products, such as CO, CO_2, O_2, as well as IBAN were analyzed by a GC-TCD equipped with packed columns (Porapak Q, 3 m length; molecular sieve 13×, 3 m length). Other products, like MAC, MAA, acetic acid (AA) and acrylic acid (ACA), were analyzed by a GC-FID equipped with an Alltech (Deerfield, IL, USA) EC1000 semi-capillary column (i.d. 0.53 mm, 30 length). The reaction data were obtained after 24 h under stream, which corresponded to steady state conditions.

4. Conclusions

The catalytic performance in the oxidation of IBAN to methacrolein and methacrylic acid being significantly improved by supporting APMV on CPM (IBAN maximum conversion of 15.3% and yield to MAA + MAC of 8.0%) the structural evolution of the catalyst was studied using various *in situ* techniques. Experiments were carried out under different atmospheres to explore the changes of the catalyst under reaction conditions. Under oxidative conditions (air), the cubic system of unsupported APMV was destroyed at temperatures higher than 400 °C. When supported on CPM, the thermal stability of APMV was significantly improved, since the Keggin structure remained unchanged until 500 °C. Under reductive atmosphere, the active phase was further stabilized up to 560 °C, and its reducibility increased. It is believed that the easier formation of V^{4+} and of Mo^{5+} species increase the catalytic activity of APMV/CPM because these species are responsible for activation of isobutane [16]. Similar observation was made by Cavani *et al.* [15], who used the ammonium salt of heteropolymolybdate, $(NH_4)_3PMo_{12}O_{40}$, in the same reaction. They found that operating at isobutane-rich (IBAN/O_2 = 26/13) instead of isobutane-lean (IBAN/O_2 = 1/13) conditions was more favorable to increase the selectivity to MAA, which reached 40% instead of 15% for similar IBAN conversion (7%–8%) after 25 h on-stream.

Concerning the decomposition mechanism of APMV, two main phenomena were evidenced by our *in situ* experiments: (I) As a consequence of the decomposition of ammonium, vanadium was eliminated from the primary structure (Keggin units) during the calcination of APMV precursor as well as during the catalytic reaction which was carried out in isobutane-lean conditions. The V species remained in the solid as mixed- valence species, V^{4+} and V^{5+}, which activated IBAN and oxidized the resulting adsorbed intermediate, respectively. The V^{5+} species could be reduced by isobutane under reaction conditions (340 °C), which is in agreement with the Mars and van-Krevelen mechanism. (II) As the product of oxidation of ammonium, ammonia was released from APMV, followed (or not, depending on temperature) by the elimination of the remaining protons as constitutional water. The addition of steam in the feed is supposed to slow down this process and maintain the specific acidity necessary for the reaction. The resulting charge disequilibrium was compensated by the migration of cesium ions from the support, forming Cs^{+}-NH_4^{+}-H^{+} mixed salts. Furthermore, it was also found that the Mo species were also partially reduced from Mo^{6+} to Mo^{5+} under reaction conditions, thus increasing the active sites since they also participate in the redox reaction. These results show that the catalyst restructures significantly under reaction conditions.

Acknowledgments

The Fonds Européen de Développement Régional (FEDER), CNRS, Région Nord Pas-de-Calais and Ministère de l'Education Nationale de l'Enseignement Supérieur et de la Recherche are acknowledged for the funding of X-ray diffractometers. Fangli Jing thanks the China Scholarship Council (CSC) for providing the financial support during his stay in France.

Author Contributions

Fangli Jing and Sébastien Paul designed the experiments. Fangli Jing performed them and wrote the paper. Benjamin Katryniok contributed to the data analysis and writing. Sébastien Paul, Franck Dumeignil and Elisabeth Bordes-Richard contributed greatly to the interpretation of results, the preparation and improvement of the manuscript.

Conflicts of Interest

The authors declare no conflict of interest.

References

1. Rao, K.N.; Srilakshmi, C.; Reddy, K.M.; Babu, B.H.; Lingaiah, N.; Prasad, P.S.S. Heteropoly Compounds as Ammoxidation Catalysts. In *Environmentally Benign Catalysts*; Patel, A., Ed.; Springer: Dordrecht, The Netherlands, 2013; pp. 11–55.
2. Ressler, T.; Dorn, U.; Walter, A.; Schwarz, S.; Hahn, A.H.P. Structure and properties of $PVMo_{11}O_{40}$ heteropolyoxomolybdate supported on silica SBA-15 as selective oxidation catalyst. *J. Catal.* **2010**, *275*, 1–10.
3. Sun, M.; Zhang, J.; Putaj, P.; Caps, V.; Lefebvre, F.; Pelletier, J.; Basset, J.M. Catalytic Oxidation of Light Alkanes (C1–C4) by Heteropoly Compounds. *Chem. Rev.* **2013**, *114*, 981–1019.

4. Enache, D.I.; Bordes, E.; Ensuque, A.; Bozon-Verduraz, F. Vanadium oxide catalysts supported on titania and zirconia: II. Selective oxidation of ethane to acetic acid and ethylene. *Appl. Catal. A* **2004**, *278*, 103–110.
5. Katryniok, B.; Paul, S.; Capron, M.; Royer, S.; Lancelot, C.; Jalowiecki-Duhamel, L.; Belliere-Baca, V.; Rey, P.; Dumeignil, F. Synthesis and characterization of zirconia-grafted SBA-15 nanocomposites. *J. Mater. Chem.* **2011**, *21*, 8159–8168.
6. Katryniok, B.; Paul, S.; Dumeignil, F. Recent Developments in the Field of Catalytic Dehydration of Glycerol to Acrolein. *ACS Catal.* **2013**, *3*, 1819–1834.
7. Brückner, A.; Scholz, G.; Heidemann, D.; Schneider, M.; Herein, D.; Bentrup, U.; Kant, M. Structural evolution of $H_4PVMo_{11}O_{40}{\cdot}xH_2O$ during calcination and isobutane oxidation: New insights into vanadium sites by a comprehensive *in situ* approach. *J. Catal.* **2007**, *245*, 369–380.
8. Song, I.; Barteau, M. Redox properties of Keggin-type heteropolyacid (HPA) catalysts: Effect of counter-cation, heteroatom, and polyatom substitution. *J. Mol. Catal. A* **2004**, *212*, 229–236.
9. Sun, M.; Zhang, J.Z.; Cao, C.J.; Zhang, Q.H.; Wang, Y.; Wan, H.L. Significant effect of acidity on catalytic behaviors of Cs-substituted polyoxometalates for oxidative dehydrogenation of propane. *Appl. Catal. A* **2008**, *349*, 212–221.
10. Paul, S.; Chu, W.; Sultan, M.; Bordes-Richard, E. Keggin-type $H_4PVMo_{11}O_{40}$-based catalysts for the isobutane selective oxidation. *Sci. Chin. Ser. B* **2010**, *53*, 2039–2046.
11. Kozhevnikov, I. Heterogeneous acid catalysis by heteropoly acids: Approaches to catalyst deactivation. *J. Mol. Catal. A* **2009**, *305*, 104–111.
12. Paul, S.; LeCourtois, V.; Vanhove, D. Kinetic investigation of isobutane selective oxidation over a heteropolyanion catalyst. *Ind. Eng. Chem. Res.* **1997**, *36*, 3391–3399.
13. Sultan, M.; Paul, S.; Fournier, M.; Vanhove, D. Evaluation and design of heteropolycompound catalysts for the selective oxidation of isobutane into methacrylic acid. *Appl. Catal. A* **2004**, *259*, 141–152.
14. Cavani, F.; Etienne, E.; Mezzogori, R.; Pigamo, A.; Trifiro, F. Improvement of catalytic performance in isobutane oxidation to methacrylic acid of Keggin-type phosphomolybdates by preparation via lacunary precursors: Nature of the active sites. *Catal. Lett.* **2001**, *75*, 99–105.
15. Cavani, F.; Mezzogori, R.; Pigamo, A.; Trifirò, F. Synthesis of methacrylic acid by selective oxidation of isobutane, catalysed by Keggin-type polyoxometalates: relationship between catalytic performance, reaction conditions and chemical–physical features of the catalyst. *C.R. Acad. Sci. Ser. IIc Chim.* **2000**, *3*, 523–531.
16. Bordes, E. The role of structural chemistry of selective catalysts in heterogeneous mild oxidation catalysis of hydrocarbons. *C.R. Acad. Sci. Ser. IIc Chim.* **2000**, *3*, 725–733.
17. Jing, F.; Katryniok, B.; Bordes-Richard, E.; Paul, S. Improvement of the catalytic performance of supported $(NH_4)_3HPMo_{11}VO_{40}$ catalysts in isobutane selective oxidation. *Catal. Today* **2013**, *203*, 32–39.
18. Jing, F.; Katryniok, B.; Dumeignil, F.; Bordes-Richard, E.; Paul, S. Catalytic selective oxidation of isobutane to methacrylic acid on supported $(NH_4)_3HPMo_{11}VO_{40}$ catalysts. *J. Catal.* **2014**, *309*, 121–135.
19. Mizuno, N.; Tateishi, M.; Iwamoto, M. Oxidation of isobutane catalyzed by $Cs_xH_{3-x}PMo_{12}O_{40}$-based heteropoly compounds. *J. Catal.* **1996**, *163*, 87–94.

20. Kozhevnikov, I.V. Sustainable heterogeneous acid catalysis by heteropoly acids. *J. Mol. Catal. A* **2007**, *262*, 86–92.
21. Jing, F.; Katryniok, B.; Dumeignil, F.; Bordes-Richard, E.; Paul, S. Catalytic selective oxidation of isobutane over $Cs_x(NH_4)_{3-x}HPMo_{11}VO_{40}$ mixed salts. *Catal. Sci. Technol.* **2014**, *4*, 2938–2945.
22. Marchal-Roch, C.; Laronze, N.; Guillou, N.; Tézé, A.; Hervé, G. Study of ammonium, mixed ammonium–cesium and cesium salts derived from $(NH_4)_5[PMo_{11}V^{IV}O_{40}]$ as isobutyric acid oxidation catalysts: Part I: Syntheses, structural characterizations and catalytic activity of the ammonium salts. *Appl. Catal. A* **2000**, *199*, 33–44.
23. Courtine, P.; Bordes, E. Mode of arrangement of components in mixed vanadia catalyst and its bearing for oxidation catalysis. *Appl. Catal. A* **1997**, *157*, 45–65.
24. Hoffman, A.; Maniv, T.; Folman, M. AES and XPS studies of no adsorption on Al(100) single crystal. *Surf. Sci.* **1987**, *183*, 484–502.
25. Lee, W.J.; Lee, Y.S.; Rha, S.K.; Lee, Y.J.; Lim, K.Y.; Chung, Y.D.; Whang, C.N. Adhesion and interface chemical reactions of Cu/polyimide and Cu/TiN by XPS. *Appl. Surf. Sci.* **2003**, *205*, 128–136.
26. Khattak, G.D.; Salim, M.A.; Al-Harthi, A.S.; Thompson, D.J.; Wenger, L.E. Structure of molybdenum-phosphate glasses by X-ray photoelectron spectroscopy (XPS). *J. Non -Cryst. Solids* **1997**, *212*, 180–191.
27. Cavani, F.; de Santi, D.; Luciani, S.; Löfberg, A.; Bordes-Richard, E.; Cortelli, C.; Leanza, R. Transient reactivity of vanadyl pyrophosphate, the catalyst for *n*-butane oxidation to maleic anhydride, in response to in-situ treatments. *Appl. Catal. A* **2010**, *376*, 66–75.
28. Khattak, G.D.; Mekki, A.; Wenger, L.E. X-ray photoelectron spectroscopy (XPS) and magnetic susceptibility studies of vanadium phosphate glasses. *J. Non-Cryst. Solids* **2009**, *355*, 2148–2155.
29. Coulston, G.W.; Thompson, E.A.; Herron, N. Characterization of VPO Catalysts by X-ray Photoelectron Spectroscopy. *J. Catal.* **1996**, *163*, 122–129.
30. Cavani, F.; Mezzogori, R.; Pigamo, A.; Trifiro, F.; Etienne, E. Main aspects of the selective oxidation of isobutane to methacrylic acid catalyzed by Keggin-type polyoxometalates. *Catal. Today* **2001**, *71*, 97–110.
31. Busca, G.; Cavani, F.; Etienne, E.; Finocchio, E.; Galli, A.; Selleri, G.; Trifiro, F. Reactivity of Keggin-type heteropolycompounds in the oxidation of isobutane to methacrolein and methacrylic acid: Reaction mechanism. *J. Mol. Catal. A* **1996**, *114*, 343–359.
32. Lee, J.K.; Russo, V.; Melsheimer, J.; Kohler, K.; Schlogl, R. Genesis of V^{4+} in heteropoly compounds $Cs_xH_{4-x}PVMo_{11}O_{40}$ during thermal treatment, rehydration and oxidation of methanol studied by EPR spectroscopy. *Phys. Chem. Chem. Phys.* **2000**, *2*, 2977–2983.